Anal Bioanal Chem
DOI 10.1007/s00216-014-8331-5

PAPER IN FOREFRONT

DI-ICR-FT-MS-based high-throughput deep metabotyping: a case study of the *Caenorhabditis elegans–Pseudomonas aeruginosa* infection model

Michael Witting · Marianna Lucio · Dimitrios Tziotis · Brigitte Wägele · Karsten Suhre · Romé Voulhoux · Steve Garvis · Philippe Schmitt-Kopplin

Received: 25 August 2014 / Revised: 20 October 2014 / Accepted: 7 November 2014

Abstract In metabolomics there is an ever-growing need for faster and more comprehensive analysis methods to cope with the increasing size of biological studies. Direct-infusion ion-cyclotron-resonance Fourier-transform spectrometry (DI-ICR-FT-MS) is used in non-targeted metabolomics to obtain high-resolution snapshots of the metabolic state of a system. We applied this technology to a *Caenorhabditis elegans–Pseudomonas aeruginosa* infection model and optimized times needed for cultivation and mass-spectrometric analysis. Our results reveal that DI-ICR-FT-MS is a promising tool for high-throughput in-depth non-targeted metabolomics. We performed whole-worm metabolomics and recovered markers of the induced metabolic changes in *C. elegans* brought about by interaction with pathogens. In this investigation, we reveal complex metabolic phenotypes enabling clustering based upon challenge. Specifically, we observed a marked decrease in amino-acid metabolism with infection by *P. aeruginosa* and a marked increase in sugar metabolism with infection by *Salmonella enterica*. We were also able to discriminate between infection with a virulent wild-type *Pseudomonas* and with an attenuated mutant, making it possible to use this method in larger genetic screens to identify host and pathogen effectors affecting the metabolic phenotype of infection.

Keywords DI-ICR-FT–MS · High-throughput deep metabotyping · Infection models · Metabolomics · *Caenorhabditis elegan*s

Introduction

Metabolomics is a widely used approach in systems biology, alongside other "omics" approaches including transcriptomics or proteomics. As the endpoint of the flow of biological information from genes to transcripts, proteins, and finally metabolites, it is the closest reflection of the observed

---

Electronic supplementary material The online version of this article (doi:10.1007/s00216-014-8331-5) contains supplementary material, which is available to authorized users.

M. Witting (✉) · M. Lucio · D. Tziotis · P. Schmitt-Kopplin (✉)
Research Unit Analytical BioGeoChemistry, Helmholtz Zentrum München, German Research Center for Environmental Health, Ingolstaedter Landstrasse 1, 85764 Neuherberg, Germany
e-mail: michael.witting@helmholtz-muenchen.de
e-mail: schmitt-kopplin@helmholtz-muenchen.de

B. Wägele
Institute of Bioinformatics and Systems Biology, Helmholtz Zentrum München, German Research Center for Environmental Health, Ingolstaedter Landstrasse 1, 85764 Neuherberg, Germany

K. Suhre
Department of Physiology and Biophysics, Weill Cornell Medical College in Qatar, P.O. Box 24144, Education City–Qatar Foundation, Doha, Qatar

R. Voulhoux · S. Garvis
Centre National de la Recherche Scientifique, 31 Chemin Joseph Aiguier, 13402 Marseille Cedex 20, France

P. Schmitt-Kopplin
Chair of Analytical Food Chemistry, Technische Universität München, Alte Akademie 10, 85354 Freising-Weihenstephan, Germany

Present Address:
S. Garvis
Laboratoire de Biologie Moléculaire de la Cellule UMR5239 CNRS/ENS Lyon/UCBL/HCL, Ecole normale supérieure de Lyon 46, Allée d'Italie, 69364 Lyon cedex 07, France

phenotype. A variety of analytical technology, including mass spectrometry (MS)—either direct infusion (DI) or hyphenated to chromatography or electrophoresis—and nuclear magnetic resonance (NMR), is used in metabolomics research. Each of these approaches has advantages and disadvantages. The most pressing challenge for future development in metabolomics is adapting to the ever-expanding number of samples to be processed in a single study, e.g. patient cohorts or large mutant screens. Often-used techniques for high-throughput metabolomics are based on direct-infusion triple-quadrupole mass spectrometry (DI-QQQ-MS), for the quantification mostly of lipids, amino acids, or carnitines. The sample is extracted together with ^{13}C-labeled compounds, and targeted mass fragmentation enables the semi-quantitative evaluation of the metabolites in a few minutes. The value of this approach has been proved in several studies [1–3]. To perform deeper analysis of an organism or system's metabolism, greater coverage of metabolites, and thus non-targeted approaches, is needed. Fuhrer et al. presented a non-targeted flow-injection-analysis time-of-flight mass spectrometer (FIA-ToF-MS) system, able to detect 3241 and 1531 ions in positive and negative-ion mode, respectively, in 1 min. This technique has been revealed to be highly reproducible, with many metabolites confirmed with authentic standards, and has been used in different studies [4, 5]. Although very competitive, annotation of ions with putative metabolites or formulas at a native resolution of 8000–12000 over the whole *m*/*z* range of 100–1000 is ambiguous. Higher resolving power of >400,000 is needed, as well as high mass accuracy to achieve unambiguous annotation or formula calculation in this mass range.

Ion-cyclotron-resonance Fourier-transform mass spectrometry (ICR-FT-MS) is an interesting alternative for overcoming the problem of resolution. ICR-FT-MS was first applied to metabolomics in 2002 by Asaph Aharoni [6]. Since then several studies have been published, with examples in different fields including plant sciences [7], wine analysis [8], and nutritional studies [9]; however, compared with LC and GC–MS or NMR, usage is still rather low. ICR-FT-MS offers ultrahigh resolution and mass accuracy together with a high-order-of-magnitude intensity range for metabolite detection. In particular, separation of different isotope species, e.g. 34S from 13C2 isotope peaks, enables more accurate annotation and/or formula calculation and can be used in labeling studies, for example [10].

The nematode *Caenorhabditis elegans* is a soil-dwelling invertebrate, and is regularly exposed to many pathogens in its natural environment. As a model organism, this genetically malleable worm has many advantages. Because the organism is hermaphroditic, large populations of genetically identical animals are easily obtained, which also results in limited variation on a metabolome level. The worm is recognized as a viable and robust model for studies in diverse fields of biology, from innate immunity to genetic regulation of aging, and for the study of host–pathogen interactions. In the laboratory *C. elegans* is routinely fed on the non-pathogenic bacteria *Escherichia coli* strain OP50, a uracil auxotroph [11], but can also be fed on a wide range of bacterial pathogens. Genome-wide transcriptomic and proteomic studies have been performed evaluating the response to a variety of bacterial pathogens [12, 13]. Metabolomic investigations of host–pathogen interactions are an emerging topic, with an increasing number of publications. For example, Müller et al. applied ICR-FT-MS and UPLC–ToF-MS to a *Chlamydia pneumoniae* infection model of HEp-2 cells [14], and Antunes et al. used ICR-FT-MS to reveal the effect of *Salmonella enterica* on the metabolome of mice [15]. However, for genetic screens of pathogen mutants affecting the host metabolome, mice are too expensive and generation time is too slow. *C. elegans*, with its short developmental cycle of 2–3 weeks, is an interesting alternative for high-throughput screening. We therefore decided to use a high-throughput, non-targeted metabolomics technique for *C. elegans* infection research based on the ultrahigh resolution of ICR-FT-MS. The two bacterial pathogens used in this study have been previously found to negatively affect the *C. elegans* life span. Nematode killing assays have been developed to identify potential bacterial virulence factors of these pathogens.

Pseudomonas aeruginosa is a ubiquitous opportunistic Gram-negative bacterium and human pathogen, able to cause infection in a wide range of hosts including animals and plants. In humans it causes localized and systemic infections of both acute and chronic nature. Previous studies with the *C. elegans* model have revealed bacterial virulence factors through both fast and slow killing assays [16, 17]. *Salmonella enterica* is a causative agent of human food-borne illness, able to enter intestinal epithelial cells and macrophages. It has been revealed that *S. enterica* is able to enter intestinal epithelial cells in *C. elegans*, and that autophagy in *C. elegans* has a protective effect [18].

Here we use this host–pathogen model coupled with direct-infusion ICR-FT-MS (DI-ICR-FT-MS) to investigate the metabolic phenotypes of *C. elegans* facing specific metabolic stresses. Short acquisition times enabled fast data collection, yielding data matrices for statistical analysis in less than a day. In this study, we reveal complex metabolic phenotypes enabling clustering based upon challenge. We identify general end-product indicators of bacterial infection within this system and specific markers for each condition, and are able to separate the fully virulent and attenuated mutant of *P. aeruginosa*. As a new, high-throughput phenotyping technology, ICR-FT-MS has great potential for use in genetic screening of bacterial pathogens in a *C. elegans* infection model.

Materials and methods

Chemicals

Methanol and water were obtained from Biosolve (Valkenswaard, The Netherlands) and were of UPLC–MS grade. All other chemicals were, at a minimum, of analytical grade. M9 buffer was prepared by dissolving 3 g KH_2PO_4, 6 g Na_2HPO_4, 5 g NaCl, and 1 mL 1 mol L^{-1} $MgSO_4$ in 1 L water and sterilized by autoclaving. Nematode growth medium (NGM) was prepared by adding 3 g NaCl, 17 g agar, and 2.5 g peptone to 975 mL water. After autoclaving for 50 min, the flask was cooled to 55 °C in a water bath for 15 min, and 25 mL 1 mol L^{-1} KH_2PO_4 buffer pH 6.0, 1 mL 5 mg mL cholesterol in ethanol, 1 mL 1 mol L^{-1} $CaCl_2$, and 1 mL 1 mol L^{-1} $MgSO_4$ were added. Luria–Bertani broth was prepared by dissolving 10 g NaCl, 10 g tryptone, and 5 g yeast extract in 1 L water, and the pH was adjusted to 7.0 with 5 mol L^{-1} NaOH.

Bacterial strains and media

The *Pseudomonas aeruginosa* strain PA14, *Salmonella enterica* serovar *Typhimurium* strain 12023, and *Escherichia coli* OP50 have been described. The *P. aeruginosa* PA14 Δ*gacA* mutant was generated using the vector pKNG101, as described in [19]. The medium for routine bacterial culture and maintenance was Luria–Bertani broth (LB). Bacteria were cultured on nematode growth medium (NGM) for nematode feeding and killing assays, as described below.

C. elegans cultivation

The nematode strains used in this work were provided by the Caenorhabditis Genetics Center, which is funded by the NIH National Center for Research Resources (NCRR). Strain *fer-15* (b26) *C. elegans* was used in this study. Worms were cultured as described in [20]. Eggs were isolated by hypochlorite treatment (“bleaching”) of gravid adults [21].

Recovered *fer-15* eggs were deposited on to non-seeded NGM plates and allowed to hatch overnight at 25 °C to obtain a synchronized population of L1-stage worms. After overnight incubation, the L1-stage population was spotted on to NGM plates seeded with OP50 and allowed to develop to late L4 at 25 °C (approximately 36 h). These worms were used in either the killing or feeding assay described below.

Feeding assay

Overnight LB broth cultures of the test bacterial strains were spread onto 9 cm diameter NGM plates and incubated at 37 °C for 24 h. Briefly, young adult hermaphrodite worms raised on *E. coli* OP50 were washed thoroughly in M9 buffer to remove residual bacteria, and 1000 worms were transferred either on to feed plates seeded with one of the bacterial cultures, or on to non-seeded plates to obtain starved worms. Plates were incubated at 25 °C for 24 h, and worms were then washed thoroughly with multiple M9 buffer changes to remove residual bacteria. After the final wash, the buffer was replaced with 1 mL 50:50 (*v*/*v*) MeOH–water and flash-frozen in liquid nitrogen.

Metabolite extraction from *C. elegans*

Extraction was similar to Geier et al., using ultrasonic extraction instead of bead beating [22]. Nematodes in MeOH–water were thawed on ice. To disrupt the worms, the mixture was sonicated for 15 min in a sonic bath with ice-cold water and vortexed every 3 to 5 min for metabolite extraction. After centrifugation at 21,000*g* for 10 min at 4 °C, the supernatant was transferred to a pre-chilled eppendorf cup, snap-frozen in liquid nitrogen, and stored in aliquots at −80 °C before analysis.

DI-ICR-FT-MS non-targeted metabolomic analysis

The metabolite extract was diluted 1:50 with 70 % MeOH before analysis. The analysis was performed on a Bruker solariX equipped with a 12 T magnet and an Apollo II ion source (Bremen, Germany). The samples were introduced with a syringe pump, at a flow of 120 μL h^{-1}. Settings for the ion source were: drying-gas temperature = 200 °C, drying-gas flow = 2.4 L min^{-1}, nebulizer-gas flow = 1.1 L h^{-1}, capillary voltage = 4500 V, spray shield = −500 V. The mass spectrometer was externally calibrated on cluster of arginine (10 mg L^{-1} in MeOH). Spectra were obtained in positive and negative-ionization mode with an *m*/*z* range from 100 to 1000 at 2 megawords and 300 scans were accumulated for one spectrum. All tubing, the syringe, and the sprayer needle were thoroughly washed between samples to prevent cross contamination of the spectra.

Data analysis of ICR-FT-MS spectra

Spectra were internally recalibrated and exported as a mass-list file (.asc) at a signal-to-noise ratio of 3, using Bruker Data Analysis 4.0 (Bremen, Germany). A matrix, containing an aligned mass list with the corresponding intensities for each sample, was generated using an in-house software tool with a window width of 1.0 ppm for peak alignment [23]. All further calculations and filtering were done in Microsoft Excel 2010. Only masses detected in four or more replicates of one biological group were kept for further statistical analysis. Hierarchical cluster analysis and generation of barplots and heatmaps were performed in R Statistical Language (version 2.13) [24]. All masses were uploaded to MassTRIX [25, 26] with a search range of 3.0 ppm for possible metabolite annotation. For mass-difference networks an in-house program was used [27]. Mass differences representing several biochemical transformations and the data matrix were used as input (Electronic Supplementary Material (ESM) Table S1). Main network graphs were visualized using yED (version 3.8, http://www.yworks.com/en/products_yed_about.html) and network characteristics were calculated using Cytoscape (version 2.8.2, http://www.cytoscape.org/).

To assess the class separation, different orthogonal partial-least-square models (OPLS/O2PLS-DA) were built in SIMCA-P 11.5 (Umetrics, Umea, Sweden). The contribution of the masses to the separation of the different groups was evaluated through examination of the different S-PLOT. Masses with the highest-magnitude covariation and correlation were chosen as potential candidates for the class separation.

Metabolite-enrichment and pathway analysis of significantly different metabolites were performed using Metaboanalyst (www.metaboanalyst.ca), Fisher's exact test was used for over-representation analysis, and pathway-topology analysis was performed using relative-betweeness centrality.

Results

Optimization of measurement, data pre-processing, and data analysis

C. elegans is a well-described model organism for many different types of study, including bacterial infections. We used an infection model consisting of several conditions, which enabled us to compare metabolic effects on the basis of feeding and/or infection. In total five different conditions were tested with biological triplicates. These samples were used to optimize the whole metabolomics procedure, from worm cultivation and pre-analytics to generation of the data matrix for statistical analysis.

The most time-limiting variable of high-throughput metabolomics is the speed of data acquisition and degree of automation. The system used enables infusion of samples using an automated liquid handler. Acquisition time and sensitivity are dependent on the number of scans acquired for one spectrum in ICR-FT-MS. In our case 300 spectra were obtained, resulting in a total acquisition time of 5–7 min, depending on the ionization mode. An additional 2–3 min are needed for washing of the transfer lines and ion source. However, depending on the extraction and matrix used, several of the washing steps can be omitted.

For our biological setup a total data-acquisition time of 5 h per ionization mode was needed for 15 samples and technical duplicates (30 injections total), with a mean time per injection of 10 min including washing time. The complete dataset used in this study was collected in less than half a day, and using complete automation overnight runs are possible.

Another important consideration for collecting high-quality data is rigorous calibration of the mass spectrometer and the obtained data. The MS was calibrated before each sample batch with 10 mg L^{-1} arginine in MeOH, and all five masses had to be detected with errors below 1 ppm. Internal recalibration of all individual spectra was performed manually with errors below 1 ppm, requiring 5 min per spectrum. Automated recalibration can be achieved by spiking known substances into the sample [15]. Exporting of spectra was automated using custom VBA scripts within Bruker Data Analysis, and alignment was performed within a 1 ppm search range using in-house software [23].

Masses found in four or more spectra per biological condition were uploaded to the metabolite-annotation server MassTRIX [25, 26]. A search against KEGG [18], HMDB [19], and LipidMaps [20] was performed, with a maximum error range of 3 ppm. Negative-mode data was corrected for the loss of a proton; positive-mode data for the attachment of a proton or sodium ion. The mean error for the annotation was 0.03 ppm for the negative mode and 0.13 ppm for the positive mode. Metabolites from different classes, including amino acids, organic and fatty acids, nucleotides, and nucleosides, could be annotated. Using this automated data evaluation, approximately 30 % of the total masses could be directly annotated with putative metabolites from different databases. The remaining non-annotated masses may correspond to neutral losses, homo or heterodimers, other adducts, or possibly novel and still unknown metabolites. Despite this, good metabolome coverage was achieved and metabolites from all major metabolic pathways could be annotated (ESM Fig. S1). To obtain additional sum formulas, mass-difference networking as described in [27] was performed, which will be discussed in a later section. Table 1 summarizes the timeframe of the different steps.

The total time from cultivation to a data matrix suitable for data analysis was 3 days and 17.4 h. Potential break points are after quenching of metabolism with cold MeOH or after extraction and sample preparation. Optimization revealed that cultivation, even with a fast-growing model organism like *C. elegans*, is the step limiting throughput, which is well known from other studies and model organisms.

The total experimental setup was optimized to obtain maximum information in as short a time as possible. This included several controls, e.g. the attenuated Δ*gacA* mutant or *S. enterica* as a different type of infection. The time needed for statistical analysis depends on the method and objectives. Our objective was to find either metabolic profiles and/or metabolites changed specifically in one condition, or a general marker for infection.

Table 1 Optimization of DI-ICR-FT-MS-based non-targeted metabolomics as a high-throughput tool for host–pathogen interaction research. Different tasks yielding a data matrix suitable for data analysis are listed with their respective time requirement

Task	Time
Sample cultivation time	3 days
(Excluding preparation of plates, etc.)	
(1000 worms per sample)	
Total time cultivation	3 days
Extraction and sample-preparation time (1000 worms per sample)	45 min per 15 samples
Dilution to appropriate concentration	15 min
Total time extraction	1 h
Mass-spectrometry measurement time	
ESI(+)	15 samples × 2 technical replicates × 10 min
ESI(−)	15 samples × 2 technical replicates × 10 min
	10 h per 120 injections
Data preprocessing I	
- Calibration and visual inspection	5 min per spectra × 120 spectra = 5 h
- Exporting	3 min
- Alignment	5 min
Data preprocessing II	
- Data filtering	30 min
- Annotation	30 min
- Mass-difference networking	30 min
Total time MS	17.4 h

Comparison of *C. elegans* fed with pathogenic and with non-pathogenic food sources

We wished to investigate further the interaction between the nematode and the bacterial pathogens on a metabolic level. To do so we established a feeding procedure allowing for the onset of bacterial infection. It was revealed that after 24 h both pathogens had established an infection; but, importantly, at this time point infected worms were still feeding normally and few worms in the population had been killed. This early-onset scheme enabled us to investigate the initial metabolic changes in the organism in response to the stressor, while minimizing the number of dead animals and the level of bacterial carry over within the gut during downstream analysis. Young adult *C. elegans fer-15 (b26)* were fed for a 24 h period on NGM plates seeded with one of the bacteria listed above. After this period of infection, the worms were washed to remove residual bacteria, quenched for metabolome analysis in cold 50:50 (*v*/*v*) MeOH–water, and snap-frozen in liquid nitrogen for storage until processing, to maintain a high level of end-product metabolites. For each experiment three independent biological replicates were produced for ICR-FT-MS analysis, and each replicate was injected twice. A data matrix was generated as described above and in the "Materials and methods section". In positive and in negative mode 11674 and 6512 masses, respectively, were detected according to our filtering rules (detection in a minimum of four of six spectra per group). To obtain a general overview of the affected metabolic pathways, masses were uploaded in a group-specific manner to MassTRIX. Masses occurring four times or more in the six spectra of a group were uploaded, and the counts of metabolites identified on a pathway were compared. Several pathways of amino-acid metabolism had lower annotation counts for stressed worms (infected or starved) than OP50-fed worms, suggesting a general reduction in this metabolism. Tattoli et al. reported that invasive bacteria induce a state of intracellular amino-acid starvation in eukaryotic cells in culture. They also found that membrane damage had a function in inducing this amino-acid-starvation state, autophagy, and changes in the TOR pathway [28]. Figure 1 shows the number of annotated metabolites in four selected pathways from amino-acid metabolism.

Non-supervised multivariate analysis reveals clear separation between feeding strategies

We used multiple non-supervised methods to summarize and find patterns in this high-dimension data. Hierarchical cluster analysis (HCA) revealed a clear separation between the five different groups. Tight clustering of biological and technical replicates revealed the high reproducibility of the approach used. Of the pathogens used, the PA14wt causes the most

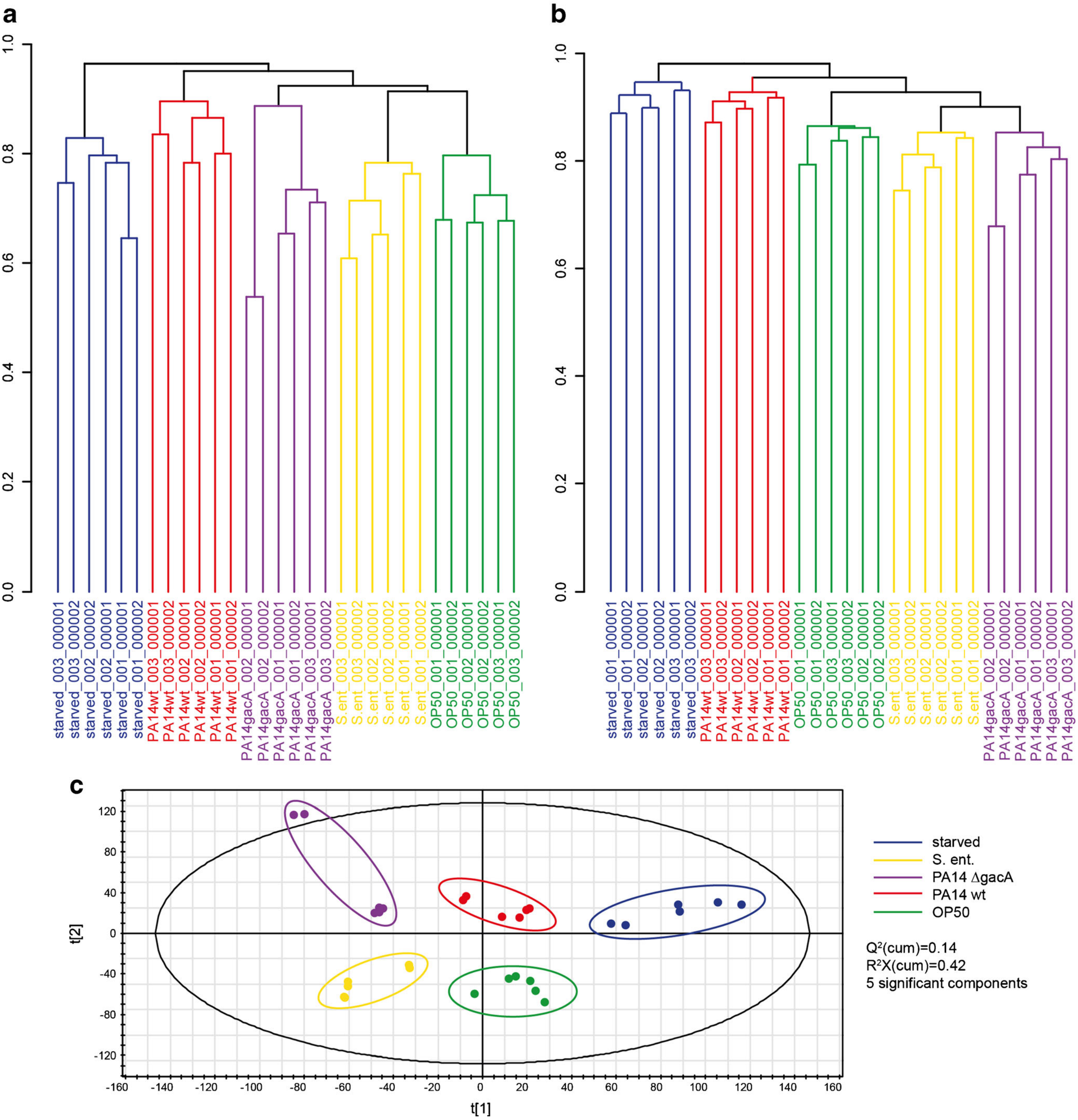

Fig. 1 (**a**) HCA of positive-ionization data shows tight clustering of biological conditions. Starvation, as a different kind of stress, is clustered away from the other conditions, and infection with the fully virulent PA14wt is different from all other feedings. (**b**) HCA of negative-ionization data, revealing similar results to positive-ionization mode. (**c**) PCA of positive-ionization data. Five significant components were identified. The first two principal components are plotted, with good separation between all groups. PC2 separates PA14wt, PA14 Δ*gacA*-infected, and starved worms from *S. enterica* and OP50-fed worms

rapid death of *C. elegans*, leading us to hypothesize that it might induce the most divergent metabolic phenotype in the model setup used. This was reflected in the results of HCA, which revealed clustering of PA14 Δ*gacA*, *S. enterica*, and OP50, with PA14wt found on a distinct branch away from this cluster. The worms undergoing starvation conditions, a very different stress from exposure to a bacterial pathogen, were also found on a separate, distinct branch. This was characterized in both ionization modes. Starvation is different from the other phenotypes tested, and the characteristic metabolome induced by non-feeding might well reflect a "minimal" metabolome the worm maintains to survive. Principalcomponent analysis also revealed good separation of all five groups: the first two principal components were able to separate all groups. Interestingly, our method is able to separate worms fed with PA14 Δ*gacA* from PA14wt-fed worms. This suggests that virulence factors regulated by GacA have a significant effect on the host metabolome. Nonetheless, the mutant is able to kill *C. elegans* more quickly than OP50. Therefore it is important both to look for metabolic markers that separate the different groups from each other, and to compare the attenuated mutant with the fully virulent wild type, to reveal metabolic changes related to bacterial pathogenicity. Figure 1 shows results obtained from unsupervised analysis.

OPLS/O2PLS-DA reveals specific metabolic patterns for each group

To enhance the identification of masses specific for each group, several OPLS/O2PLS-DA models were constructed comparing one group with the remaining groups; for example, OP50-fed *C. elegans* versus all others (ESM Fig. S2 and Fig. S3, Tables S2 and S3). Several known and unknown metabolites were found to be significantly different between the groups. As an illustration of this, degradation products of phenylalanine including phenylpyruvate, phenyllactate, and 2-hydroxy-3-phenylpropanoate were found to be significantly higher in OP50-fed worms than in worms in the other feeding schemes. This is in agreement with the counts of annotated metabolites on the phenylalanine-metabolism pathway as indicated above. Surprisingly, several metabolites of this pathway that are not produced by *C. elegans* were found, including trans-cinnamate or trans-3-hydroxycinnamate. Investigating the same pathway for *E. coli*, it was revealed that this bacteria is capable of producing this metabolite. The pathway map in Fig. 2c shows a representative diagram of phenylalanine metabolism, with markers for OP50-fed nematodes mapped in green and metabolites not found to be important for any group in gray. Metabolites and enzymes in the green frame are possibly of bacterial origin. According to the KEGG database, *P. aeruginosa* and *S. enterica* are also unable to synthesize these metabolites. Consistent with this, these metabolites were not detected in these samples. In conclusion, these metabolites probably originate from ingested OP50 or from attached bacteria remaining after washing. The other pathways depicted in Fig. 1c were also checked for this situation. In these metabolic pathways most of the enzymes present in *C. elegans* can also be found in the other three organisms, so within this study setup it is not possible to specifically determine the origins of common metabolites.

To examine the effect of infection on amino-acid metabolism, levels of all detected amino acids were compared. Evaluating the levels of different detected amino acids revealed that OP50-fed worms usually have higher levels than worms fed with the highly attenuated PA14 Δ*gacA* mutant. In general, amino-acid levels are lower in worms fed with PA14wt than in PA14 Δ*gacA* or OP50-fed worms, with the exception of glutamate and tryptophan. Tryptophan is a precursor of serotonin, one of the four biogenic amine neurotransmitters in *C. elegans*. However, there was no difference in 5-hydroxy-l-tryptophan and serotonin between PA14 Δ*gacA* and PA14wt. The same is true for the kynurenine-degradation pathway. In a NMR-based study of bacterial infection in mice it was revealed that levels of tryptophan, and of lysine, threonine, valine, and phenylalanine, correlated with the number of bacteria in the mouse serum. These amino acids were also increased in bacterial metabolomic footprints of *P. aeruginosa* obtained in the same study. The authors suggest that the elevated levels in serum are directly derived from excreted amino acids [29]. Tryptophan metabolites have been also described in regulation of the type III secretion system, and excretion of tryptophan [30] and other metabolites is possibly part of a complex signaling system.

As well as amino acids, important energy metabolites were investigated. Again, comparing levels of these metabolites in OP50 and PA14 Δ*gacA*-fed worms revealed significant differences, revealing the value of the mutant control. *C. elegans* infected with PA14wt have lower levels of acetyl-coenzyme A, citrate and/or isocitrate, cis-aconitate, 2-oxoglutarate, succinate, and malate than the PA14 Δ*gacA* control, suggesting lower activity of the TCA cycle in infected worms. Starved worms also have lower levels of these metabolites. In contrast, the *S. enterica* group has levels similar to the PA14 Δ*gacA* group. OP50-fed worms have varying levels. Figure 3 shows barplots for these metabolites. A recent study of *Drosophila* infected with *Listeria monocytogenes* also found significant effects on general energy metabolism [31].

To reveal additional pathways affected during infection, metabolite-enrichment analysis was performed. For this purpose, metabolites found to be significant for one group were uploaded to Metaboanalyst (www.metaboanalyst.ca), and enrichment and pathway analysis was performed [32]. *P*-values were calculated by Fisher's exact test. However, only for *S. enterica*-fed worms were significant enrichments found. Masses revealed to be significant for this group by OPLS/O2PLS-DA were mapped to different sugar-metabolism pathways, as shown in Fig. 3.

Taken together, it could be seen that *S. enterica*-fed worms have a different energy metabolism from PA14wt-infected worms, supporting the theory of a specific metabolic reaction upon infection with different bacterial species. A recent study by Antunes et al. revealed a great effect on energy metabolism of mice upon infection with *S. enterica*, and major changes in host hormone metabolism [15].

Overall several masses have been found to be characteristic for each group, possibly reflecting a metabolic signal of infected worms. Heatmaps of all characteristic masses

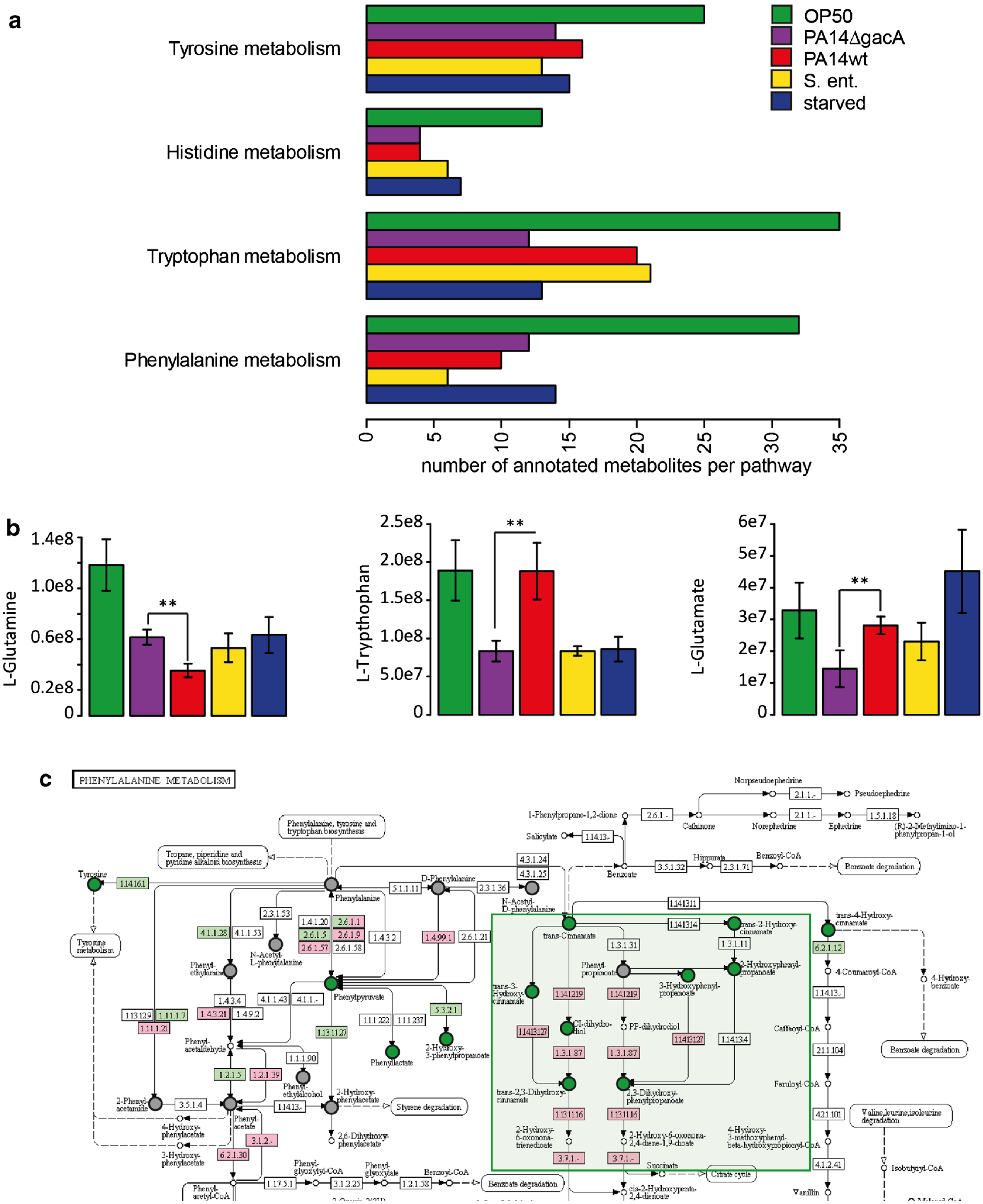

obtained by the different OPLS/O2PLS-DA models from both ionization modes can be found in the ESM (Fig. S4 and Fig. S5), revealing unique markers for each group. However, the amount of significant different masses is overwhelmingly

◀ **Fig. 2** (**a**) Pathway profile of four of the major pathways affected by stress, showing number of annotated metabolites on the respective pathway for each group. Masses occurring four or more times per group were uploaded to the MassTRIX webserver and the different samples were compared at the pathway level. (**b**) Several amino acids were detected in positive-ionization mode. All except tryptophan and glutamate have lower levels in worms fed with *P. aeruginosa*. Different levels may derive from nutritional differences between the different bacteria. (**c**) Pathway map of phenylalanine metabolism (cel00360). Metabolites found to be significant for OP50-fed worms by OPLS/O2PLS-DA are marked in *green. Gray* metabolites are not specific for any group. Results by group-specific annotation using MassTRIX were validated by OPLS/O2PLS-DA showing phenylalanine metabolites to be significant for *E. coli* OP50-fed worms. Metabolites in the *green frame* may be of bacterial origin, because *C. elegans* lacks enzymes for their synthesis

high and most have no putative annotation. To further evaluate these unknowns, novel techniques to transform them to a (bio)chemical entity are needed.

Network-based formula calculation adds novel putative formulas to unknown masses

As noted, several masses found to be significantly different between the groups have no putative annotation. To further evaluate these unknown masses, network-based formula calculation was performed as described in [27]. The method is based on mass differences between exact masses. Mass differences between all possible combinations of experimental masses are calculated, and compared within a specific error range against theoretical mass differences of biochemical reactions; for example, a mass difference of 18.01056 Da corresponds to loss or gain of H_2O. Several mass differences were tested, and an optimum set was computed (data not shown) and is shown in ESM Table S1. In total 1184 and 778 additional formulas for positive and negative-ionization mode, respectively, could be annotated in addition to the MassTRIX formulas in the main network. Several subnetworks disconnected from the main graph exist, suggesting that the input mass differences may be incomplete or insufficient to cover all metabolic transformations or for novel unknown mass transformations. Only basic transformations, for example oxidation, can be represented in mass differences; special cases including condensation or cleavage reaction are not amenable to this approach. Figure 4 shows the obtained networks for positive and negative-ionization mode, and network characteristics for the main network are shown in ESM Fig. S6. These characteristics reveal that the calculated formulas are not random, as described before by Tziotis et al. for natural organic matter. The network approach can be used to link unknown masses to known metabolites via exact mass differences, as revealed by, for example, Walker et al. [33, 34]. Using this approach a putative formula ($[C_{23}H_{37}NO_7P]^-$) could be annotated to mass 470.23136 ($[M-H]^-$), detected in negative-ionization mode, and found to be significantly higher in PA14wt and *S. enterica*-fed worms. When comparing the mass spectra with a simulated isotopic pattern, a good match between the putative formula and the true spectra was obtained (Fig. 4d). This mass was closely connected by a mass difference corresponding to the difference formulas of C2H4 and C4H8, suggesting a potential homologous series of similar molecules may exist. No matching metabolites could be found in the databases used for annotation, but the occurrence in all measured samples strongly suggests a biological relevance for *C. elegans*. Deriving a full structure from a formula is still not possible, but these formulas enable searches in chemical databases, for example PubChem or Chemspider.

Discussion

Timeframe of experiments using ICR-FT-MS

We optimized our non-targeted metabolomics approach using DI-ICR-FT-MS with a representative set of samples from a *C. elegans* infection model. Times for each step from cultivation to creation of the final data matrix were evaluated. Typical measurement times for optimized ICR-FT-MS analysis range from 5 to 10 min. In our case 300 scans for one spectrum was found to be the optimum compromise between sensitivity and throughput, yielding measurement times of 5 to 7 min depending on the ionization mode. An additional 3 min are needed for extensive washing steps to avoid cross contamination. In this work we used very extensive washing of the transfer capillary and ESI needle, but different tests have revealed that reducing the washing steps to 50 % iPrOH alone still significantly reduces carry over between samples (data not shown). We could identify two steps limiting throughput in our approach. First, cultivation of samples is the most time-consuming step in the setup and cannot be reduced. Although smaller amounts of worms can be probably used (see following sections), generation and development times are the limiting factors. However, compared with other animal models, for example the mouse model, the time required is reasonably fast for high-throughput screening. The second limiting step is the data recalibration, which is the most time-consuming data-processing step. We did not spike standard substances for automated calibration, but other groups have revealed that this works well [15, 35]. Bruker Data Analysis enables the writing of custom scripts for automated data processing. Additionally, new software developments, e.g. Genedata Expressionist for MS, offer workflow-based processing of raw data, including recalibration. Recalibration is crucial to successful use of DI-ICR-FT-MS to utilize the high resolving power and mass accuracy.

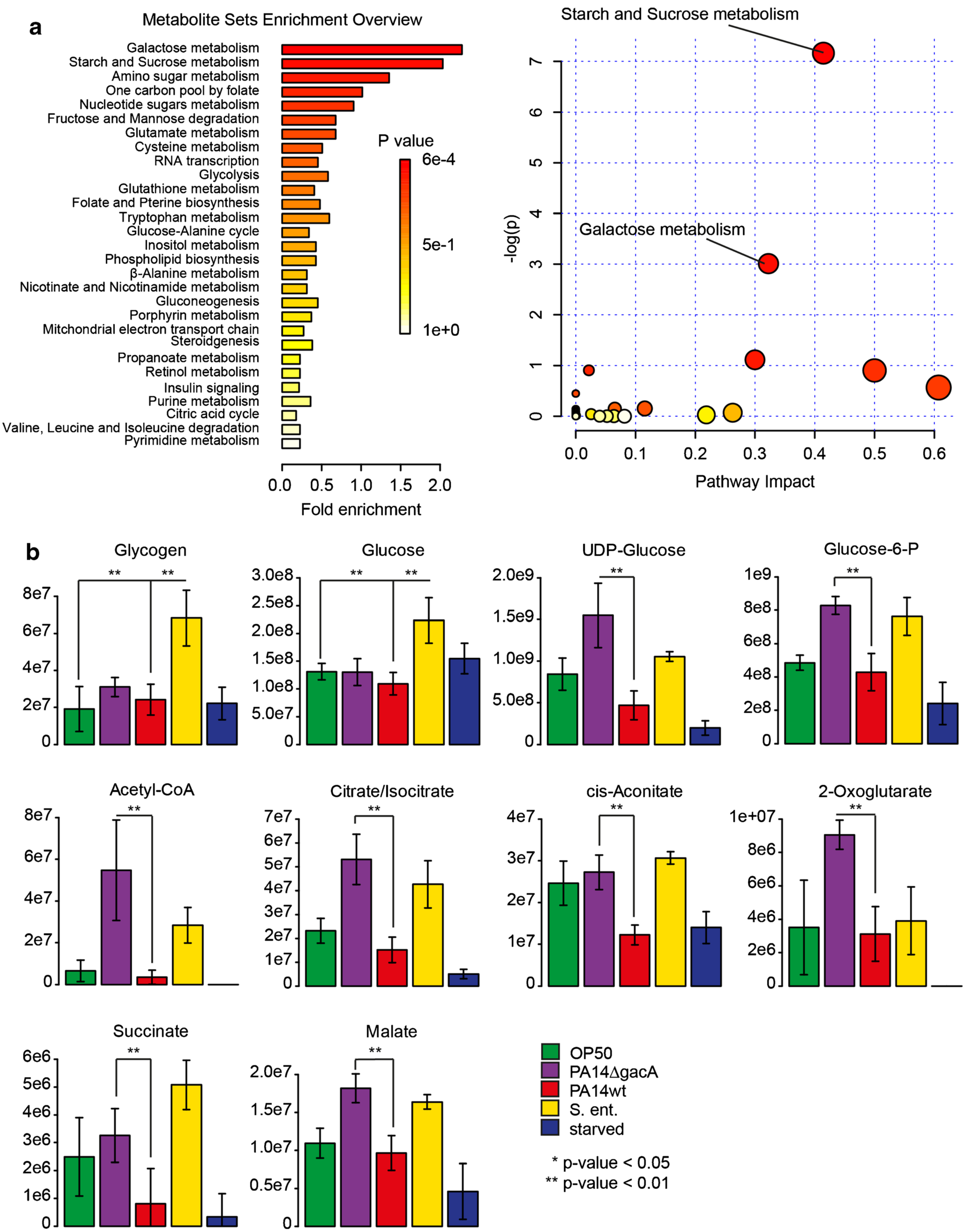
a
Metabolite Sets Enrichment Overview
Galactose metabolism
Starch and Sucrose metabolism
Amino sugar metabolism
One carbon pool by folate
Nucleotide sugars metabolism
Fructose and Mannose degradation
Glutamate metabolism
Cysteine metabolism
RNA transcription
Glycolysis
Glutathione metabolism
Folate and Pterine biosynthesis
Tryptophan metabolism
Glucose-Alanine cycle
Inositol metabolism
Phospholipid biosynthesis
β-Alanine metabolism
Nicotinate and Nicotinamide metabolism
Gluconeogenesis
Porphyrin metabolism
Mitchondrial electron transport chain
Steroidgenesis
Propanoate metabolism
Retinol metabolism
Insulin signaling
Purine metabolism
Citric acid cycle
Valine, Leucine and Isoleucine degradation
Pyrimidine metabolism
0.0 0.5 1.0 1.5 2.0
Fold enrichment
P value
6e-4
5e-1
1e+0
Starch and Sucrose metabolism
Galactose metabolism
-log(p)
0 1 2 3 4 5 6 7
0.0 0.1 0.2 0.3 0.4 0.5 0.6
Pathway Impact
b
Glycogen
0 2e7 4e7 6e7 8e7
Glucose
0 5.0e7 1.0e8 1.5e8 2.0e8 2.5e8 3.0e8
UDP-Glucose
0 5.0e8 1.0e9 1.5e9 2.0e9
Glucose-6-P
0 2e8 4e8 6e8 8e8 1e9
Acetyl-CoA
0 2e7 4e7 6e7 8e7
Citrate/Isocitrate
0 1e7 2e7 3e7 4e7 5e7 6e7 7e7
cis-Aconitate
0 1e7 2e7 3e7 4e7
2-Oxoglutarate
0 2e6 4e6 6e6 8e6 1e+07
Succinate
0 1e6 2e6 3e6 4e6 5e6 6e6
Malate
0 0.5e7 1.0e7 1.5e7 2.0e7
**
🟩 OP50
🟪 PA14ΔgacA
🟥 PA14wt
🟨 S. ent.
🟦 starved
* p-value < 0.05
** p-value < 0.01

◀ **Fig. 3** (**a**) Metabolites obtained by the OPLS/O2PLS-DA were subjected to Metaboanalyst for enrichment and pathway analysis. The enrichment analysis revealed that galactose, starch, and sucrose and the amino-sugar metabolism are significantly enriched. The pathway analysis takes the centrality of a metabolite into account; in this analysis galactose, starch, and sucrose metabolism also have significant values. (**b**) Of the different detected storage and energy metabolites, most were significantly lower in PA14wt-fed *C. elegans* than PA14 Δ*gacA*. Compared with all other groups, *S. enterica*-fed worms have higher levels of glycogen, glucose, and glucose-6-phosphate, suggesting higher use of energy from sugar stores. Levels of TCA-cycle metabolites were comparable to PA14 Δ*gacA* or *E. coli* OP50. The starvation group has generally low levels of these metabolites and the PA14wt-group levels are similar to the starvation ones, suggesting a similar metabolic phenotype

Compared with other high-throughput approaches, we were able to generate an in-depth picture of the *C. elegans* metabolome during infection. Targeted approaches, for example the Biocrates technique, enable detection of 180 metabolites, mostly from lipid metabolism, in 5 min, which is a similar timeframe to that needed for our analysis. The big advantage of that technique is that it provides quantitative data. However, DI-ICR-FT-MS can be also used for quantification by the use of correct internal standards [35]; for example, the standard-addition approach [36]. If the matrix is kept constant, ion-suppression effects can be assumed to be comparable between samples and semi quantification is possible.

High-level throughput was achieved by the FIA-ToF-MS system presented by Fuhrer et al. [4]. They focused on hydrophilic substances of the central metabolism. In contrast, we used 50 % MeOH for extraction, which gives a broader overview of metabolites and even small lipids. In both studies not all ions could be annotated with putative annotations, indicating that both approaches may enable discovery of novel metabolites. Because of higher resolving power and mass accuracy, the ICR-FT-MS approach enables very precise direct calculation of molecular

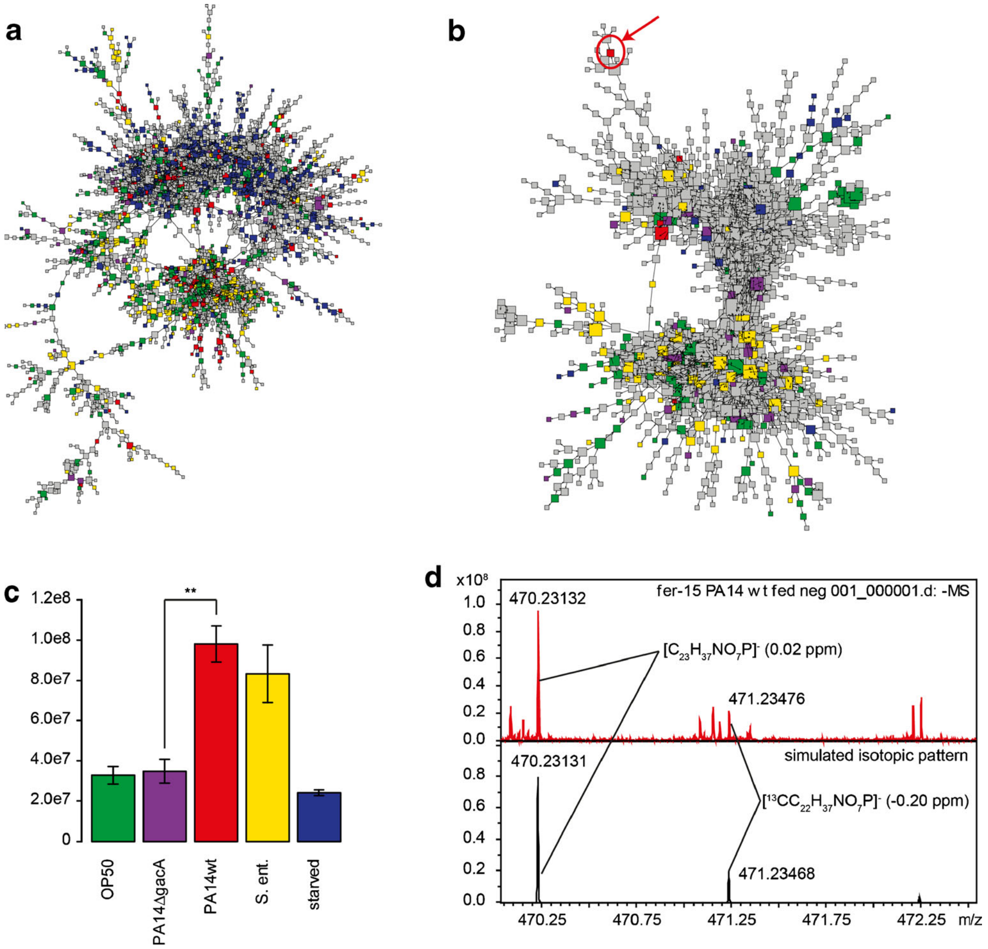

Fig. 4 Mass-difference networks of metabolite datasets. (**a**) Main network created on the basis of the mass differences in ESM Table S1 for positive-ionization mode. (**b**) Main network for negative-ionization mode. Nodes in both plots are colored on the basis of the results of OPLS/O2PLS-DA. *Green* nodes are specific for *E. coli* OP50-fed *C. elegans*, *red* for *P. aeruginosa* PA14wt, *violet* for *P. aeruginosa* PA14 Δ*gacA*, *yellow* for *S. enterica*, and *blue* for starved. *Gray* nodes are non-specific masses. The *red circle* and *red arrow* indicate the position of mass 470.23136 in the network. Size of nodes corresponds to centrality of the mass in the network. Mass-difference networks enable annotation of possible molecular formulas beyond the annotation process using databases. (**c**) Barplot of mass 470.23136, which is significantly higher in *C. elegans* fed with fully virulent pathogens. (**d**) Mass spectra from one PA14wt-fed *C. elegans* sample zoomed to mass range of the unknown compound in (**c**), shown with the simulated isotopic pattern of the corresponding molecular formula

formulas for unknowns, e.g. using mass-difference-based formula calculation. The main advantage of this high resolving power is the differentiation of different isotopic peaks, e.g. ^{34}S from $^{13}C_2$.

Compared with other methods used in metabolomics, for example UHPLC–MS or GC–MS, DI-ICR-FT-MS is superior regarding time needed for analysis and comprehensiveness of analysis. As we report, several thousands of features can be detected in a short time. Ballistic gradients <5 min for high throughput can be used in UHPLC–MS-based metabolomics, but this technique can only partially resolve metabolites or overlapping isotopic patterns. A further advantage of DI-ICR-FT-MS is a good stability over time; this is because there is no use of chromatography, where, e.g., deterioration of the column material can lead to changes in separation. Maintenance in DI-ICR-FT-MS is limited to regular cleaning of the ESI spray chamber and all fluidic connections, whereby contamination is kept very low because of the use of highly diluted samples. Although DI-ICR-FT-MS has high initial costs, the time saving and comprehensiveness of results mean this method is comparable with standard (commercial) techniques including UHPLC–MS regarding per-sample costs.

Non-targeted metabolomics using DI-ICR-FT MS reveals specific metabolic phenotypes in *C. elegans* infection

Our metabolomics-based experimental setup is able to separate *Pseudomonas aeruginosa* PA14-infected worms from non-infected worms, can distinguish infection from other stresses, and can even discriminate between different strains or pathogens on a molecular level. This is as far as we are aware the first time ICR-FT-MS-based metabolic profiling has been applied to a *C. elegans* infection. The inclusion of the PA14 Δ*gacA* was an important control because it revealed changes related to the full virulence of *P. aeruginosa* and differences in the metabolome based on contact with specific bacterial pathogens. Previous work in this field has focused on identifying virulence genes or regulated genes in the host response. With our approach it is possible to obtain the overall effect of both, with the metabolism as the endpoint of all these actions in the host. We found reduced metabolites of energy metabolism in PA14wt-infected worms compared with the other infections (PA14 Δ*gacA* and *S. enterica*). Additionally, several unknown metabolites correlated with pathophysiological states of infection or starvation; e.g., mass 470.23136 ($[M-H]^-$) was found to be significantly elevated in infection with fully virulent bacteria. Using mass-difference-network-based formula calculation we were able to putatively annotate this mass with the formula $[C_{23}H_{37}NO_7P]^-$, which suggests a lipid-like structure. Future investigations will have the objective of purifying and identifying this and other unknown metabolites from crude *C. elegans* extracts. Although our direct-infusion approach cannot separate different isomers, it provides a working hypothesis for further targeted analysis.

DI-ICR-FT-MS as a high-throughput metabolomics tool for *C. elegans* infection research

With our setup we were able to generate a comprehensive metabolite profile for different conditions in a reasonably short time. Cultivation of *C. elegans* is the major step limiting throughput in this setup. We were able to separate the fully virulent wild type from the highly attenuated *gacA* mutant of *P. aeruginosa*. GacA is a master regulator upstream of several virulence factors, and it is therefore not clear which virulence factor is responsible for the observed metabolic phenotype. However, we have revealed that our technique is able to handle samples in a high-throughput manner, with the possibility of measuring >120 samples per day. We would especially like to emphasize the final concentration and amount of sample needed for analysis with ICR-FT-MS. One sample containing 1000 worms was extracted with 1 mL 50 % MeOH and further diluted to 1:50, yielding an effective concentration of 20 worms per milliliter. The effective volume for 5 min of measurement is 10 μL, but actual consumption is much higher as a result of syringe size. Use of direct-infusion nanoelectrospray sources can further reduce the volume needed for analysis [37, 38]. Using microtiter plate-based cultivation currently amounts to roughly 100 worms, which can be grown in one well [39]. Therefore larger screening regimes of different *P. aeruginosa* mutants or other pathogens are possible to reveal molecules causing changes in the host's metabolome, which can afterwards be examined in a targeted manner.

Conclusion

We have revealed that DI-ICR-FT-MS is a valuable tool that enables non-targeted metabolomics in high-throughput metabolic profiling of *C. elegans* infection models, with broad metabolome coverage. We could identify metabolic phenotypes specific to the different nutrition and infection conditions. The differences obtained between worms fed with a highly attenuated PA14 Δ*gacA* mutant and its parental strain PA14wt indicates our approach could be used to screen for changes directly linked to deletion of specific bacterial virulence genes when compared with the wild type. As a high-throughput tool in *C. elegans* infection research, it enables the forward selection of interesting mutants of host and/or pathogen for further targeted analysis, e.g. using UPLC–MS and/or NMR.

Acknowledgments The authors would like to thank Thomas Rattei for the excellent leadership of the Pathomics project and suggestions to pathogen–host metabolomics.

The study was funded by German Federal Ministry of Education and Research in the frame of the ERA-NET project “Pathogen-host metabolomics and interactomics (Pathomics)” (0315442C).

References

1. Menni C, Zhai G, MacGregor A, Prehn C, Römisch-Margl W, Suhre K, Adamski J, Cassidy A, Illig T, Spector T, Valdes A (2013) Targeted metabolomics profiles are strongly correlated with nutritional patterns in women. Metabolomics 9(2):506–514. doi:10.1007/s11306-012-0469-6
2. Altmaier E, Emeny RT, Krumsiek J, Lacruz ME, Lukaschek K, Häfner S, Kastenmüller G, Römisch-Margl W, Prehn C, Mohney RP, Evans AM, Milburn MV, Illig T, Adamski J, Theis F, Suhre K, Ladwig K-H (2013) Metabolomic profiles in individuals with negative affectivity and social inhibition: a population-based study of Type D personality. Psychoneuroendocrinology 38(8):1299–1309. doi:10.1016/j.psyneuen.2012.11.014
3. Jourdan C, Linseisen J, Meisinger C, Petersen A-K, Gieger C, Rawal R, Illig T, Heier M, Peters A, Wallaschofski H, Nauck M, Kastenmüller G, Suhre K, Prehn C, Adamski J, Koenig W, Roden M, Wichmann HE, Völzke H (2014) Associations between thyroid hormones and serum metabolite profiles in an euthyroid population. Metabolomics 10(1):152–164. doi:10.1007/s11306-013-0563-4
4. Fuhrer T, Heer D, Begemann B, Zamboni N (2011) High-throughput, accurate mass metabolome profiling of cellular extracts by flow injection–time-of-flight mass spectrometry. Anal Chem 83(18): 7074–7080. doi:10.1021/ac201267k
5. Heux S, Fuchs T, Buhmann J, Zamboni N, Sauer U (2012) A high-throughput metabolomics method to predict high concentration cytotoxicity of drugs from low concentration profiles. Metabolomics 8(3):433–443. doi:10.1007/s11306-011-0386-0
6. Aharoni A, Ric de Vos CH, Verhoeven HA, Maliepaard CA, Kruppa G, Bino R, Goodenowe DB (2002) Nontargeted metabolome analysis by use of fourier transform ion cyclotron mass spectrometry. OMICS J Integr Biol 6(3):217–234
7. Kaling M, Kanawati B, Ghirardo A, Albert A, Winkler JB, Heller W, Barta C, Loreto F, Schmitt-Kopplin P, Schnitzler J-P (2014) UV-B mediated metabolic rearrangements in poplar revealed by non-targeted metabolomics. Plant Cell Environ. doi:10.1111/pce.12348
8. Roullier-Gall C, Lucio M, Noret L, Schmitt-Kopplin P, Gougeon RD (2014) How subtle is the "terroir" effect? chemistry-related signatures of two "climats de bourgogne". PLoS ONE 9(5):e97615. doi:10.1371/journal.pone.0097615
9. Daniel H, Gholami AM, Berry D, Desmarchelier C, Hahne H, Loh G, Mondot S, Lepage P, Rothballer M, Walker A, Bohm C, Wenning M, Wagner M, Blaut M, Schmitt-Kopplin P, Kuster B, Haller D, Clavel T (2014) High-fat diet alters gut microbiota physiology in mice. ISME J 8(2):295–308. doi:10.1038/ismej.2013.155
10. Gläser K, Kanawati B, Kubo T, Schmitt-Kopplin P, Grill E (2014) Exploring the Arabidopsis sulfur metabolome. Plant J 77(1):31–45. doi:10.1111/tpj.12359
11. Brenner S (1974) The Genetics of Caenorhabditis elegans. Genetics 77(1):71–94
12. Irazoqui JE, Troemel ER, Feinbaum RL, Luhachack LG, Cezairliyan BO, Ausubel FM (2010) Distinct Pathogenesis and Host Responses during Infection of C. elegans by P. aeruginosa and S. aureus. PLoS Pathog 6(7):e1000982. doi:10.1371/journal.ppat.1000982
13. Irazoqui JE, Urbach JM, Ausubel FM (2010) Evolution of host innate defence: insights from Caenorhabditis elegans and primitive invertebrates. Nat Rev Immunol 10(1):47–58
14. Müller C, Dietz I, Tziotis D, Moritz F, Rupp J, Schmitt-Kopplin P (2013) Molecular cartography in acute Chlamydia pneumoniae infections—a non-targeted metabolomics approach. Anal Bioanal Chem 405(15):5119–5131. doi:10.1007/s00216-013-6732-5
15. Antunes LCM, Arena ET, Menendez A, Han J, Ferreira RBR, Buckner MMC, Lolić P, Madilao LL, Bohlmann J, Borchers CH, Finlay BB (2011) Impact of salmonella infection on host hormone metabolism revealed by metabolomics. Infect Immun 79(4):1759–1769. doi:10.1128/iai. 01373-10
16. Tan M-W, Mahajan-Miklos S, Ausubel FM (1999) Killing of Caenorhabditis elegans by Pseudomonas aeruginosa used to model mammalian bacterial pathogenesis. Proc Natl Acad Sci U S A 96(2): 715–720
17. Garvis S, Munder A, Ball G, de Bentzmann S, Wiehlmann L, Ewbank JJ, Tümmler B, Filloux A (2009) Caenorhabditis elegans semi-automated liquid screen reveals a specialized role for the chemotaxis gene cheB2 in pseudomonas aeruginosa virulence. PLoS Pathog 5(8):e1000540
18. Jia K, Thomas C, Akbar M, Sun Q, Adams-Huet B, Gilpin C, Levine B (2009) Autophagy genes protect against Salmonella typhimurium infection and mediate insulin signaling-regulated pathogen resistance. Proc Natl Acad Sci 106(34):14564–14569. doi:10.1073/pnas.0813319106
19. Kaniga K, Delor I, Cornelis GR (1991) A wide-host-range suicide vector for improving reverse genetics in Gram-negative bacteria: inactivation of the blaA gene of Yersinia enterocolitica. Gene 109(1):137–141. doi:10.1016/0378-1119(91)90599-7
20. Lewis JA, Fleming JT (1995) Chapter 1 Basic Culture Methods. In: Henry FE, Diane CS (eds) Methods in Cell Biology, vol Volume 48. Academic Press, pp 3–29. doi:10.1016/s0091-679x(08)61381-3
21. Porta-de-la-Riva M, Fontrodona L, Villanueva A, Cer NJ (2012) Basic caenorhabditis elegans methods: synchronization and observation. J Vis Exp 64:e4019. doi:10.3791/4019
22. Geier FM, Want EJ, Leroi AM, Bundy JG (2011) Cross-platform comparison of caenorhabditis elegans tissue extraction strategies for comprehensive metabolome coverage. Anal Chem 83(10):3730–3736. doi:10.1021/ac2001109
23. Lucio M, Fekete A, Frommberger M, Schmitt-Kopplin P (2011) Metabolomics: high-resolution tools offer to follow bacterial growth on a molecular level. In: Handbook of molecular microbial ecology I. John Wiley & Sons, Inc., pp 683–695. doi:10.1002/9781118010518.ch72
24. R Core Team (2012) R: a language and environment for statistical computing. R Foundation for Statistical Computing, Vienna, Austria. http://www.R-project.org/
25. Suhre K, Schmitt-Kopplin P (2008) MassTRIX: mass translator into pathways. Nucleic Acids Res 36(suppl 2):W481–W484
26. Wägele B, Witting M, Schmitt-Kopplin P, Suhre K (2012) MassTRIX reloaded: combined analysis and visualization of transcriptome and metabolome data. PLoS One 7(7):e39860. doi:10.1371/journal.pone.0039860
27. Tziotis D, Hertkorn N, Schmitt-Kopplin P (2011) Kendrick-analogous network visualisation of ion cyclotron resonance Fourier transform mass spectra: improved options for the assignment of elemental compositions and the classification of organic molecular complexity. Eur J Mass Spectrom 17(4):6
28. Tattoli I, Sorbara MT, Vuckovic D, Ling A, Soares F, Carneiro Leticia AM, Yang C, Emili A, Philpott Dana J, Girardin Stephen E (2012) Amino acid starvation induced by invasive bacterial pathogens triggers an innate host defense program. Cell Host Microbe 11(6):563–575. doi:10.1016/j.chom.2012.04.012
29. Hoerr V, Zbytnuik L, Leger C, Tam PPC, Kubes P, Vogel HJ (2012) Gram-negative and gram-positive bacterial infections give rise to a different metabolic response in a mouse model. J Proteome Res 11(6):3231–3245. doi:10.1021/pr201274r
30. Shen D-K, Filopon D, Chaker H, Boullanger S, Derouazi M, Polack B, Toussaint B (2008) High-cell-density regulation of the Pseudomonas aeruginosa type III secretion system: implications for tryptophan catabolites. Microbiology 154(8):2195–2208. doi:10.1099/mic. 0.2007/013680-0
31. Chambers MC, Song KH, Schneider DS (2012) *Listeria monocytogenes* infection causes metabolic shifts in *Drosophila melanogaster*. PLoS ONE 7(12):e50679. doi:10.1371/journal.pone.0050679

32. Xia J, Mandal R, Sinelnikov IV, Broadhurst D, Wishart DS (2012) MetaboAnalyst 2.0—a comprehensive server for metabolomic data analysis. Nucleic Acids Res. doi:10.1093/nar/gks374
33. Walker A, Pfitzner B, Neschen S, Kahle M, Harir M, Lucio M, Moritz F, Tziotis D, Witting M, Rothballer M, Engel M, Schmid M, Endesfelder D, Klingenspor M, Rattei T, Castell W, de Angelis MH, Hartmann A, Schmitt-Kopplin P (2014) Distinct signatures of host-microbial meta-metabolome and gut microbiome in two C57BL/6 strains under high-fat diet. ISME J. doi:10.1038/ismej.2014.79
34. Walker A, Lucio M, Pfitzner B, Scheerer MF, Neschen S, de Angelis MH, Hartmann A, Schmitt-Kopplin P (2014) Importance of sulfur-containing metabolites in discriminating fecal extracts between normal and type-2 diabetic mice. J Proteome Res. doi:10.1021/pr500046b
35. Han J, Danell R, Patel J, Gumerov D, Scarlett C, Speir J, Parker C, Rusyn I, Zeisel S, Borchers C (2008) Towards high-throughput metabolomics using ultrahigh-field Fourier transform ion cyclotron resonance mass spectrometry. Metabolomics 4(2):128–140
36. Krajewski MP, Kanawati B, Fekete A, Kowalski N, Schmitt-Kopplin P, Grill E. Analysis of Arabidopsis glutathione-transferases in yeast. Phytochemistry (0). doi:10.1016/j.phytochem.2012.04.016
37. Southam AD, Payne TG, Cooper HJ, Arvanitis TN, Viant MR (2007) Dynamic range and mass accuracy of wide-scan direct infusion nanoelectrospray fourier transform ion cyclotron resonance mass spectrometry-based metabolomics increased by the spectral stitching method. Anal Chem 79(12):4595–4602. doi:10.1021/ac062446p
38. Erve JCL, DeMaio W, Talaat RE (2008) Rapid metabolite identification with sub parts-per-million mass accuracy from biological matrices by direct infusion nanoelectrospray ionization after clean-up on a ZipTip and LTQ/Orbitrap mass spectrometry. Rapid Commun Mass Spectrom 22(19):3015–3026. doi:10.1002/rcm.3702
39. Solis GM, Petrascheck M (2011) Measuring caenorhabditis elegans life span in 96 well microtiter plates. (49):e2496. doi:10.3791/2496

Michael Witting analytical chemist by teaching and postdoctoral fellow at the Research Unit Analytical BioGeoChemistry, is interested in developing new approaches in metabolomics and lipidomics research and their application to *C. elegans* under different states of health and disease.

Marianna Lucio's expertise is related to statistical analysis and data mining for metabolomics data. Her main interest is the applications and the investigation of different chemometrics methods to extrapolate meaningful biological knowledge from the data.

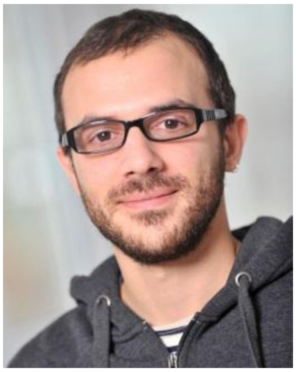

Dimitrios Tziotis is developing data-analysis methods for analysis of ultrahigh-resolution mass-spectrometry data using mass-difference and compositional networks for calculating molecular formulas.

Brigitte Wägele is interested in metabolite annotation and pathway analysis and is responsible for the metabolite-annotation server MassTRIX.

Karsten Suhre is a Professor of Biophysics and Physiology at Weill Cornell Medical College and the director of the Bioinformatics Core at its branch campus in Qatar. His research interest is genomics and metabolomics of complex disorders and of hereditary diseases.

Romé Voulhoux trained as a molecular bacteriologist and works at the LISM CNRS Aix-Marseille Université (http://lism.cnrs-mrs.fr/) where he leads the group "Secretion Systems and Pathogenicity in *Pseudomonas aeruginosa*". His principal research topic is the type II secretion system (T2SS), of which he tries to understand the functioning.

Steve Garvis is a researcher in the group of F. Palladino at the LBMC ENS-Lyon, where they study epigenetic regulation in development using the *C. elegans* model. His research interest is organismal response to stress.

Philippe Schmitt-Kopplin's research efforts focus on the chemodiversity analysis (metabolomics) of complex bio(geo)systems and/or microbiomes and the study of generic biotic and abiotic processes in biology and the geosphere. This can be achieved with (ultra)-high-resolution analytical tools enabling the targeted and non-targeted analysis of complex mixtures. The focus is developing non-invasive approaches and identifying new active compounds and biomarkers in health and environment.